Rapid Multiplex Ultrafast Nonlinear Microscopy for Advanced Material Characterization

Torben L. Purz,[1] Blake T. Hipsley,[1] Eric. W. Martin,[2] Ronald Ulbricht,[3] and Steven T. Cundiff[1,2,*]

[1] *University of Michigan, Department of Physics, Ann Arbor, Michigan 48104, USA*
[2] *MONSTR Sense Technologies, LLC, Ann Arbor, Michigan 48108, USA*
[3] *Max Planck Institute for Polymer Research, Ackermannweg 10, 55128 Mainz, Germany*

[*] *cundiff@umich.edu*

Abstract: We demonstrate rapid four-wave mixing (FWM) imaging to assess the quality of emerging optical and electronic materials. We show that FWM intensity, dephasing times, and excited state lifetimes are accurate sample quality indicators.

As new groups of semiconductor materials shift into focus, the need to image these materials for fundamental science and to characterize them at scale has spurred numerous experimental innovations. These materials include two-dimensional quantum materials such as transition metal dichalcogenides (TMDs) and graphene, III-V semiconductors such as gallium arsenide and gallium nitride, and silicon carbide. Material characterization of TMDs and other advanced materials has seen a plethora of techniques, from white-light optical microscopy to photoluminescence imaging, Raman spectroscopy, atomic force microscopy imaging, and more. However, these techniques either convey little information about the material quality or require complicated experimental setups, potentially involving tens of minutes to hours of data acquisition.

To overcome the limitations of existing techniques, we here introduce rapid multiplex ultrafast nonlinear imaging, enabled by recent advances in lock-in detection [1], to characterize advanced materials. Our approach is based on heterodyne-detected four-wave mixing (FWM) generated by three pulses impinging on the sample. We acquire FWM intensity images, dephasing maps, and exciton population lifetime maps using the scheme outlined in Ref. 2. The presented technique employs degenerate FWM, which has a high sensitivity to defects and interfaces due to its scaling with material oscillator strength. Moreover, dephasing times are a measure of the systems temporal coherence [3], crucial for many quantum information applications. Additionally, exciton population lifetimes (or, more generally, pump-probe decay times) are a good indicator of sample quality as they have previously proven useful in defect sensing [4]. We demonstrate the technique's feasibility on a WSe_2 monolayer grown by chemical vapor deposition (CVD), which serves as a canonical example.

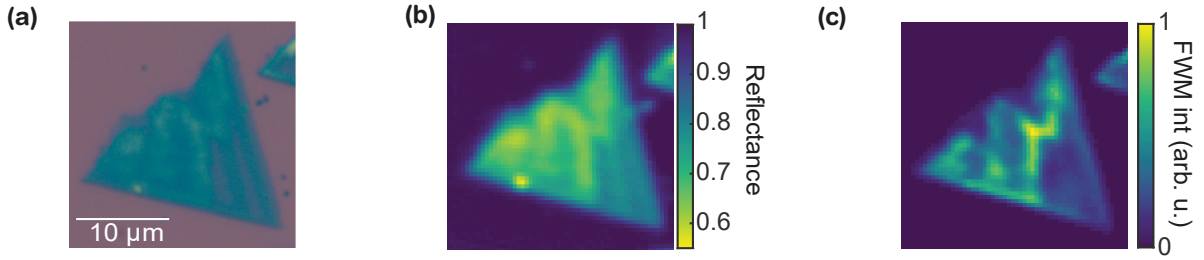

Fig. 1. **(a)** White-light microscopy image (false color) of a CVD-grown WSe_2 monolayer. **(b)** Resonant integrated reflectance from 1600 meV to 1700 meV of the WSe_2 monolayer. Here, we set the substrate to have a reflectance of one. **(c)** FWM intensity image of the WSe_2 monolayer.

Fig. 1 shows a comparison of white-light (Fig. 1(a)), resonant reflectance (Fig. 1(b)), and FWM microscopy (Fig. 1(c)). In the white light microscopy image, the monolayer shows an uneven structure due to residue remaining from the transfer process. However, none of this information allows for drawing conclusions about the actual material properties. The resonant (with the exciton) integrated reflectance image gives limited access to the sample's dipole moment and density of states and thus provides more information than white-light microscopy. Nonetheless, no definite conclusions about the sample's properties can be drawn from this measurement. In comparison, the FWM image in Fig. 1(c) has a much-enhanced contrast. It also provides complementary information to the linear reflectance image - while some areas of decreased reflectance show an increased FWM, some areas of decreased reflectance also show a reduced FWM. The key element behind this is the FWMs sensitivity to

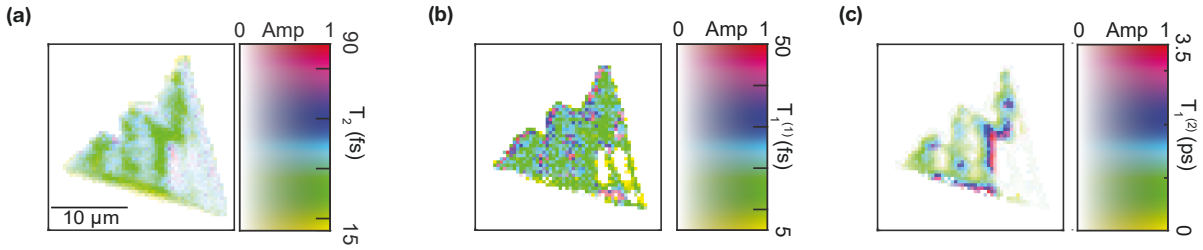

Fig. 2. **(a)** Dephasing time T_2 map of the sample obtained by fitting a uni-exponential decay in the time domain. The hue level signifies the dephasing time, while the saturation signifies the FWM strength. **(b)** Fast decay component (amplitude and time $T_1{}^{(1)}$) of the exciton population lifetime. **(c)** Slow decay component (amplitude and time $T_1{}^{(2)}$) of the exciton population lifetime.

local strain profiles, changes in the dielectric environment, doping, trapped charges, impurities, defect densities, and distribution of dark states [3]. Most importantly, however, the FWM image identifies regions with uniquely distinct material properties, as evident from the dephasing and lifetime maps plotted in Fig. 2.

Fig. 2(a) shows a joint representation of FWM intensity and dephasing times. Here, the hue level signifies the dephasing times, while the saturation signifies the FWM intensity. The high FWM intensity area of the sample shows homogeneous dephasing times across the sample, except for the bottom part, which shows faster dephasing. However, several low FWM areas on the sample show a significantly increased dephasing time. The increased apparent dephasing times are an artifact from fitting curves that are not mono-exponential decays with a simple exponential. The non-exponential behavior arises from many-body effects, which results in a delayed rise of the signal [2]. Nevertheless, the rapid dephasing imaging technique still uniquely identifies the areas of increased many-body effects. We have also confirmed the accuracy of the extracted dephasing times in regions of low many-body effects by comparing them with dephasing times extracted from multidimensional coherent spectroscopy [2].

For the exciton population lifetime images in Fig. 2(b,c), we fit a bi-exponential decay to the data to capture the full temporal decay dynamics of the WSe_2 flake, which displays rapid, sub-50 fs decay, followed by a slower decay on the order of a few picoseconds. The amplitude of the first decay component is relatively homogeneous across the sample, while the decay time fluctuates mainly between 10-25 fs, approximately twice as fast as the dephasing time. These observations suggest a radiatively limited dephasing time via the relation $T_2 = 2T_1$. Although we observe a factor between 1.5-2 in our measurements, this deviation can be explained by the dephasing and decay times approaching the temporal resolution of the experimental setup. The second decay component shows a more distinct spatial profile, matching the spatial intensity profile of the FWM plotted in Fig. 1(c). The bottom and center of the sample display a longer decay time on the order of 2-3 ps, while the rest of the sample shows decay times of around 1 ps. Bi-exponential decays for monolayer TMDs have been observed in the past, with the fast component being attributed to the population relaxation of bright excitons and the second decay component attributed to additional states such as dark states or localized states beyond a simple two-level system [5]. In this case, the fast decay is caused by a decay into the dark states. After exciton populations of bright and dark states equilibrate, excitons tunneling back from dark into bright states, and subsequent radiative decay of the bright excitons causes the slow decay of the signal. The population lifetime maps are thus an indirect probe of the dark state distribution, an identifier of pristine areas of the sample.

In summary, these results constitute an important step toward real-time material characterization of advanced materials on an industrial scale, a necessity for devices to make it out of the lab and into the marketplace.

References

1. T. L. Purz, S. T. Cundiff, and E. W. Martin, "Lock-in detector for accelerated nonlinear imaging," Opt. Lett. **46**, 4813–4816 (2021).
2. T. L. Purz, B. T. Hipsley, E. W. Martin, R. Ulbricht, and S. T. Cundiff, "Rapid multiplex ultrafast nonlinear microscopy for material characterization," arXiv:2208.06633 (2022).
3. T. L. Purz, E. W. Martin, W. G. Holtzmann, P. Rivera, A. Alfrey, K. M. Bates, H. Deng, X. Xu, and S. T. Cundiff, "Imaging dynamic exciton interactions and coupling in transition metal dichalcogenides," The J. Chem. Phys. **156**, 214704 (2022).
4. K.-C. Huang, J. McCall, P. Wang, C.-S. Liao, G. Eakins, J.-X. Cheng, and C. Yang, "High-speed spectroscopic transient absorption imaging of defects in graphene," Nano Lett. **18**, 1489–1497 (2018). PMID: 29342361.
5. G. Moody, C. Kavir Dass, K. Hao, C.-H. Chen, L.-J. Li, A. Singh, K. Tran, G. Clark, X. Xu, G. Berghäuser, E. Malic, A. Knorr, and X. Li, "Intrinsic homogeneous linewidth and broadening mechanisms of excitons in monolayer transition metal dichalcogenides," Nat Commun **6**, 8315 (2015).